



SACLANT ASW
RESEARCH CENTRE
REPORT

MODEL FOR THE FREQUENCY SPREAD OF BACKSCATTERED UNDERWATER SOUND
BASED ON THE FACET MODEL OF THE ROUGH SEA SURFACE

by

HERWARD SCHWARZE

1 NOVEMBER 1978

NORTH
ATLANTIC
TREATY
ORGANIZATION

LA SPEZIA, ITALY

This document is unclassified. The information it contains is published subject to the conditions of the legend printed on the inside cover. Short quotations from it may be made in other publications if credit is given to the author(s). Except for working copies for research purposes or for use in official NATO publications, reproduction requires the authorization of the Director of SACLANTCEN.

This document is released to a NATO Government at the direction of the SACLANCEN subject to the following conditions:

1. The recipient NATO Government agrees to use its best endeavours to ensure that the information herein disclosed, whether or not it bears a security classification, is not dealt with in any manner (a) contrary to the intent of the provisions of the Charter of the Centre, or (b) prejudicial to the rights of the owner thereof to obtain patent, copyright, or other like statutory protection therefor.

2. If the technical information was originally released to the Centre by a NATO Government subject to restrictions clearly marked on this document the recipient NATO Government agrees to use its best endeavours to abide by the terms of the restrictions so imposed by the releasing Government.

SACLANTCEN REPORT SR-26

NORTH ATLANTIC TREATY ORGANIZATION

SACLANT ASW Research Centre
Viale San Bartolomeo 400, I-19026 San Bartolomeo (SP), Italy
Tel: (0187)503540
Telex: 28148

MODEL FOR THE FREQUENCY SPREAD OF BACKSCATTERED UNDERWATER SOUND
BASED ON THE FACET MODEL OF THE ROUGH SEA SURFACE

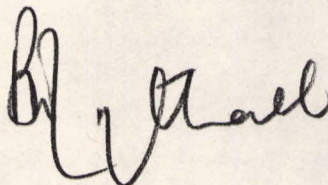
by

Herward Schwarze

[Reprinted from *Jnl Acoustical Society America* 64, 1978: 605-613]

1 November 1978

APPROVED FOR DISTRIBUTION



B.W. LYTHALL
Director

Model for the frequency spread of backscattered underwater sound based on the facet model of the rough sea surface

Herward Schwarze^{a)}

SACLANT ASW Research Center, I-19100 La Spezia, Italy
(Received 2 March 1976; revised 1 May 1978)

A theoretical model for the Doppler spread of backscattered acoustic waves from the rough sea surface is described on the basis of the decomposition of the continuous sea-surface spectrum that leads to the concept of facets. The facet statistics are derived for a Gaussian sea surface. The results are evaluated for a Pierson-Moskowitz spectrum. A procedure for choosing the facet length is developed. Approximate, simple formulas for the Pierson-Moskowitz case are given. The general result for the Doppler spread of the backscattered acoustic wave is evaluated for sea-surface spectrum due to Scott, and examples for Doppler spectra are given for different windspeeds, wind directions, grazing angles, and acoustic frequencies.

PACS numbers: 43.30.Gv, 43.30.Cq

INTRODUCTION

The important problem of scattering of acoustic waves from the rough-moving sea surface has often been investigated, but a general, exact, and tractable solution has not yet been obtained.

For special cases, solutions are known, e.g., for the cases where the amplitudes of the sea-surface waves are much smaller¹ or much larger² than the length of the incident wave.

For arbitrary roughness of the sea surface, approximate solutions are obtained by applying the small-scale backscattering results to a composite-roughness sea-surface model.³⁻⁶ This means that the small waves with lengths up to some 10 cm, causing the resonant or "Bragg" scattering, are carried by long waves. The long waves are approximated by plane facets whose movements depend on the large-scale roughness of the sea surface.

In this paper, the interest is focused on the frequency spreading of a backscattered monochromatic acoustic plane wave. This case is of special interest in active sonar applications, because the moving sea surface limits the detectability of slowly moving targets.

The presentation given here contains nearly no derivations of the resulting formulas, the proofs of which can be found in Ref. 7.

I. RESONANT BACKSCATTERING THEORY FOR SMALL SEA-SURFACE ROUGHNESS

The geometry shown in Fig. 1 is used. A source $S(x_0, 0, z_0)$ illuminates a surface area $A = ab$ with a plane wave of frequency f_0 and pressure amplitude p_0 . The distance r_0 is considered much larger than $A^{1/2}$.

Without loss of generality the y coordinate of S is set to zero. Besides the specular reflection, the rough sea surface causes a scattered field in all directions. For backscattering, source S and receiver R coincide.

The Doppler spectrum $\Phi(f)$ of the backscattered wave $p(t)$ is the Fourier transform of its correlation function; viz,

$$\Phi(f) = \int_{-\infty}^{+\infty} E[p^*(t)p(t+T)] \exp(-2\pi j f T) dT. \quad (1)$$

A normalization is introduced, yielding a backscattering Doppler density

$$\varphi(f) = \Phi(f) r_0^2 / p_0^2 A. \quad (2)$$

Following Clarke,⁸ for example, the basic equation for the backscattering Doppler density for the slightly rough sea surface is

$$\varphi(f) = (4\pi)^2 \sin^4 \gamma_0 k_0^4 X_3(-2k_0 \cos \gamma_0, 0, f - f_0) \quad (3)$$

or

$$\begin{aligned} \varphi(f) = & (2g^2 k_0^4 \sin^4 \gamma_0 / f_0^3) F_2(f_0^*, 0) \\ & \times [W(f_0^*, \pi) \delta(f - f_0 - f_0^*) + W(f_0^*, 0) \delta(f - f_0 + f_0^*)], \end{aligned} \quad (4)$$

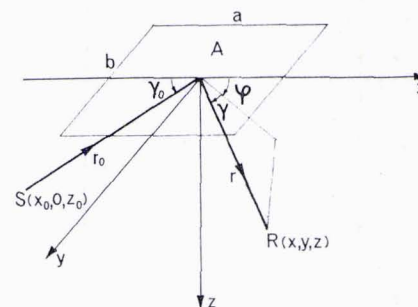


FIG. 1. Geometry for scattering from the sea surface.

^{a)}Present address: Fachhochschule Bielefeld, D-4800 Bielefeld 1, Federal Republic of Germany.

where

$$f_0^* = (gk_0 \cos \gamma_0 / \pi)^{1/2} \quad (5)$$

is the dispersion relation and k_0 is explained in the Appendix.

When integrated over f , Eqs. (3) and (4) become the backscattering strength known from the literature.^{5,9} Equations (3) and (4) are considered to be valid under the following conditions:

(1) $\lambda_0 \gg 2\pi \sin \gamma_0 \sigma_h$, "Bragg" scattering, Rayleigh theory,¹⁰ where σ_h is the standard deviation of the sea-surface height.

(2) $\lambda_0 \ll A^{1/2}$, an implicit assumption for Eqs. (3) and (4).

(3) $r_0 \gg A^{1/2}$, the assumption of an incident plane wave.

(4) $1/k > 0.05$ m, an approximate rule for the validity of the dispersion relation, Eq. (A3). As most acoustic wavelengths in sonar applications are between 0.1 and 1 m, condition (1) is often not fulfilled. One possible way to find results that approximate the rough-sea-surface case is to introduce the composite sea-surface model which circumvents the condition. This model is developed in the Sec. II.

II. DOPPLER SPECTRUM FOR A COMPOSITE-ROUGHNESS SEA SURFACE

The facet model assumes basically a two-component structure of the rough-moving sea surface: The small-scale high-frequency roughness (ripples), responsible for the resonant scattering, are carried by the low-frequency large-scale sea-surface waves (swell). These carrier waves are locally approximated by plane facets of finite extent. The movements of the facets have influences on the backscattering strength and the Doppler shifts of the backscattered sound.

It is emphasized that the facet model is an approximation and is meant in an empirical sense. It makes certain assumptions and neglects certain difficulties that are mentioned below. First of all, it is a statistical model and considers not a single facet but a large number of facets. Thus it requires that the facet dimensions are much smaller than the insonified area of the sea surface. The optimal choice of the facet dimensions remains as an unsolved problem. Considerations that lead to a practical choice are found in Sec. IIB. Further on the division of the continuous sea-surface spectrum into a large and a small roughness regime is somewhat arbitrary. There exists a part in the spectrum that is intermediate and is not treated in the facet model. It is believed that this part is of small influence as the energy compared to the large-scale roughness part is small, but this is not proved and the question is open to further investigation.

A. Facet statistics

The facets are statistically described by a five-dimensional random process: The variables are the inclinations ϵ_x and ϵ_y and the velocities u_x , u_y , and u_z

in the appropriate coordinate directions. Bearing in mind that the incident acoustic wave vector lies in the x - z plane, the following two simplifying assumptions are made that reduce the mathematical effort considerably:

(1) The contribution of the facet velocity u_y , that is perpendicular to the acoustic wave vector, to the Doppler shift of the backscattered frequency is considered small and neglected.

(2) The facet slope ϵ_y is neglected with the argument that the amount of energy scattered out of the x - z plane because of a slope ϵ_y will be scattered back into this plane by other facets, lying outside the x - z plane and having the slope $-\epsilon_y$, such that the effects cancel.

These simplifications reduce the process to a three-dimensional one, and the facet is represented by a straight line. As it is assumed that the sea surface is described as a Gaussian process, the facet movement is also considered to be normally distributed. The mean values of the stochastic variables $\epsilon = \epsilon_x(t)$, $u_x(t)$, and $u_z(t)$ are zero by definition. Therefore, the covariance matrix is sufficient for their complete description. The geometry shown in Fig. 2 is used. To obtain an expression for the facet slope $\epsilon(t)$ and the facet height $b(t)$, the sea-surface function $h(x, y, t)|_{y=0}$ is approximated by a least-square-error straight line,

$$f(x, t) = \epsilon(t)x + b, \quad (6)$$

in the interval $|x| \leq \frac{1}{2}L$. This yields

$$\epsilon(t) = \frac{12}{L^3} \int_{-(1/2)L}^{+(1/2)L} xh(x, y, t) dx \quad (7)$$

and

$$b(t) = \frac{1}{L} \int_{-(1/2)L}^{+(1/2)L} h(x, y, t) dx. \quad (8)$$

The vertical velocity u_z follows from Eq. (8)

$$u_z(t) = \frac{\partial b(t)}{\partial t} = \frac{1}{L} \int_{-(1/2)L}^{+(1/2)L} \frac{\partial h(x, y, t)}{\partial t} dx. \quad (9)$$

For the horizontal velocity u_x the following argument applies. From the linear theory of surface waves it follows that the horizontal particle velocity u in the x direction is

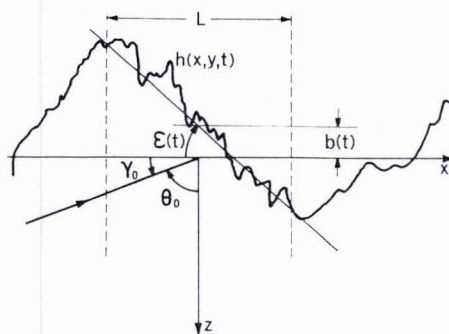


FIG. 2. Facet description.

$$\frac{\partial u}{\partial t} = -g \frac{\partial h(x, y, t)}{\partial x} \quad (10)$$

The horizontal velocity of the facet u_x is defined as the mean particle velocity on the facet

$$u_x(t) = \frac{1}{L} \int_{-(1/2)L}^{+(1/2)L} u dx \quad (11)$$

Inserting Eq. (10) into Eq. (11) gives

$$u_x(t) = -\frac{g}{L} \int_{t_0}^t [h(\frac{1}{2}L, y, t_1) - h(-\frac{1}{2}L, y, t_1)] \times dt_1 + u_x(t_0) \quad (12)$$

From Eqs. (7), (9), and (11) the variances and cross variances of the facet movement are calculated. The results are given in terms of the frequency angle spectrum $F_2(f, \varphi)$ of the sea surface. The relation of $F_2(f, \varphi)$ to the covariance function $C(x, y, \tau)$ of the sea surface is seen from the Appendix.

It is

$$\sigma_\epsilon^2 = \frac{144}{L^6} \int_{-\pi/0}^{+\pi/\infty} \int_{-\pi/0}^{+\pi/\infty} \frac{F_2(f, \varphi)}{a^4} \times (La \cos \frac{1}{2}aL - 2 \sin \frac{1}{2}aL)^2 df d\varphi \quad (13)$$

$$\sigma_z^2 = \frac{2g^2}{L^2} \int_{-\pi/0}^{+\pi/\infty} \int_{-\pi/0}^{+\pi/\infty} \frac{F_2(f, \varphi)(1 - \cos aL)}{(2\pi f \cos \varphi)^2} df d\varphi \quad (14)$$

$$\sigma_x^2 = \frac{2g^2}{L^2} \int_{-\pi/0}^{+\pi/\infty} \int_{-\pi/0}^{+\pi/\infty} \frac{F_2(f, \varphi)(1 - \cos aL)}{(2\pi f)^2} df d\varphi \quad (15)$$

$$\sigma_{\epsilon z} = \frac{-12}{L^3} \int_{-\pi/0}^{+\pi/\infty} \int_{-\pi/0}^{+\pi/\infty} F_2(f, \varphi) [2W(f, \varphi) - 1] 2\pi f \times [- (\sin aL/a^2) + (2/La^3)(1 - \cos aL)] df d\varphi \quad (16)$$

and

$$E_\epsilon \{ \epsilon u_x \} = E_\epsilon \{ u_x u_z \} = 0 \quad (17)$$

where

$$a = (2\pi f)^2 \cos \varphi / g \quad (18)$$

B. Choice of the facet length

The facet statistics as derived in the preceding section depend entirely on the facet length L . In practical cases, this L has to be chosen. The choice is directed by two influences. Firstly, the facet length should be greater than the wave length of the incident acoustic wave to reduce the error induced by the margin of the facet. That leads to the condition

$$L_{\min} \gg \lambda_0 \quad (19)$$

Secondly, the sea-surface roughness $\sigma_h(L)$ on the facet should be much smaller than the acoustic wave length λ_0 to fulfill the Rayleigh condition,

$$\lambda_0 \gg \sigma_h(L_{\max}) \quad (20)$$

It is pointed out that the facet theory itself does not predict an optimal facet length L , therefore the procedure

of choosing L developed here is one among other possibilities. It maximizes a quality number N , introduced by the equations

$$L = \lambda_0 N \quad (21)$$

and

$$\lambda_0/N = \sigma_h(L) \quad (22)$$

Combining them gives

$$L \sigma_h(L) = \lambda_0^2 \quad (23)$$

This implicit equation has to be solved to find the facet length L . The number N shows, how far L is away from the limits where the conditions for the validity of the composite sea surface model are not longer fulfilled. If N is less than about 2, this indicates that the facet model will not yield correct results.

To solve Eq. (23), an expression for $\sigma_h(L)$ has to be found. It is

$$\sigma_h^2 = E \left\{ \frac{1}{L} \int_{-(1/2)L}^{+(1/2)L} [h(x, y, t)|_{y=0} - \epsilon(t)x - b(t)]^2 dx \right\} \quad (24)$$

which can be shown to be

$$\sigma_h^2(L) = \int_{-\pi/0}^{+\pi/\infty} \int_{-\pi/0}^{+\pi/\infty} F_2(f, \varphi) \left\{ 1 - \frac{4}{a^2 L^2} \left[\left(1 - \frac{6}{a^2 L^2} \right) \cos aL - \frac{6}{aL} \sin aL + 2 + \frac{6}{L^2 a^2} \right] \right\} df d\varphi \quad (25)$$

With Eq. (25) it is possible to solve Eq. (23) by an iterative procedure for practical cases where $F_2(f, \varphi)$ is known explicitly. This will be investigated in Sec. III.

C. Doppler spectrum

The Doppler spectrum for a rough sea surface takes into account the facet movements whose statistics were described in the preceding chapter. The grazing angle γ_0 and the incident frequency f_0 are modulated by the facet inclination $\epsilon(t)$ and the facet velocities $u_x(t)$ and $u_z(t)$, respectively, and accordingly the small scale result in Eq. (4) is changed. The modulation changes γ_0 and f_0 to statistic variables of the following form:

(1) Influence of the facet slope,

$$\gamma_f(t) = \gamma_0 + \epsilon(t) \quad (26)$$

(2) Influence of the facet velocities,

$$f_f(t) = f_0 + (2f_0/c) \times [u_z(t) \sin \gamma_f(t) - u_x(t) \cos \gamma_f(t)] \quad (27)$$

To obtain the backscattered Doppler density $\varphi(f)$, the weighted sum for all ϵ , u_x , and u_z has to be taken. Using Eq. (4) one finds

$$\varphi(f) = 2g^2 \iiint_{-\infty}^{+\infty} \frac{k_{0f}^4 \sin^4 \gamma_f}{f_f^{*3}} F_2(f_f^*, 0) \times [W(f_f^*, \pi) \delta(f - f_f - f_f^*) + W(f_f^*, 0) \delta(f - f_f + f_f^*)] \times w_3(\epsilon, u_z, u_x) d\epsilon du_z du_x \quad (28)$$

This integral can be solved in closed form for a small

facet slope ϵ . The general formula for the doppler density $\varphi(f)$ is

$$\begin{aligned} \varphi(f) = & \left(\frac{\pi^3 g \cos^5 \gamma_0}{c^3} \right)^{1/2} \frac{1}{4 f_0 \sin \gamma_0} \\ & \times [(f - f_0^*)^{5/2} F_2(f_0^*, 0) W(f_0^*, \pi) L_- \\ & + (f + f_0^*)^{5/2} F_2(f_0^*, 0) W(f_0^*, 0) L_+], \end{aligned} \quad (29)$$

where

$$f_{*,+}^* = [g \cos \gamma_0 (f \mp f_0) / \pi c]^{1/2} \quad (30)$$

and

$$\begin{aligned} L_{-,+} = & w(u_{-,+}, 0, \sigma_1) [3\sigma_\epsilon^4 (1 - \rho_{\epsilon z}^2)^2 \\ & + 6\sigma_\epsilon^2 (1 - \rho_{\epsilon z}^2) (\sigma_z^2 + m_{-,+}^2) + 3\sigma_z^4 + 6\sigma_z^2 m_{-,+}^2 + m_{-,+}^4]. \end{aligned} \quad (31)$$

In Eq. (31) the abbreviations are

$$u_{-,+} = (f - f_0 \mp f_0^*) c / 2 f_0 \sin \gamma_0, \quad (32)$$

$$\sigma_1 = (\sigma_x^2 + \sigma_z^2 \tan^2 \gamma_0)^{1/2} / \tan \gamma_0, \quad (33)$$

$$\sigma_2 = \frac{\sigma_\epsilon \sigma_x \rho_{\epsilon x}}{(\sigma_x^2 + \sigma_z^2 \tan^2 \gamma_0)^{1/2}} = \frac{\sigma_x \sigma_\epsilon}{\sigma_1 \tan \gamma_0}, \quad (34)$$

and

$$m_{-,+} = \frac{\sigma_\epsilon \sigma_z \rho_{\epsilon z} u_{-,+} \tan^2 \gamma_0}{\sigma_x^2 + \sigma_z^2 \tan^2 \gamma_0} + \tan \gamma_0. \quad (35)$$

The general result of Eq. (29) has been programmed on

$$\sigma_\epsilon^2 = \frac{\alpha v^4}{\beta x_n L^2 g^2} \int_0^\pi \cos^n(\varphi - \varphi_0) \left\{ \frac{18}{u_0^2} + \frac{48}{u_0^4} + \cos u_0 \times \left(-1 + \frac{6}{u_0^2} - \frac{48}{u_0^4} \right) + \sin u_0 \left(u_0 - \frac{2}{u_0} - \frac{48}{u_0^3} \right) - u_0^2 \text{Ci}(|u_0|) \right\} d\varphi, \quad (40)$$

$$\begin{aligned} \sigma_z^2 = & \frac{2\alpha v^2}{3\beta^{1/2}} \int_0^\pi \cos^n(\varphi - \varphi_0) \\ & \times \left\{ 1 + \cos u_0 \left(\frac{1}{2} - 1/u_0^2 \right) + \sin u_0 / (2u_0 + \frac{1}{2} |u_0| \text{Si}(|u_0|)) \right\} d\varphi, \end{aligned} \quad (41)$$

$$\begin{aligned} \sigma_x^2 = & \frac{2\alpha v^6}{3\beta^{1.5} x_n L^2 g^2} \int_0^\pi \cos^n(\varphi - \varphi_0) \\ & \times \left\{ 1 + \cos u_0 \left(-1 + \frac{1}{2} u_0^2 \right) + \frac{1}{2} u_0 \sin u_0 + \frac{1}{2} |u_0|^3 \text{Si}(|u_0|) \right\} d\varphi, \end{aligned} \quad (42)$$

and

$$\begin{aligned} \rho_{\epsilon z} = & \frac{12(1 - 2W_0) \alpha v^3}{\beta^{0.75} x_n L g} \int_{\varphi_w - \pi/2}^{\varphi_w + \pi/2} \cos^n(\varphi - \varphi_0) \\ & \times \left\{ \sin u_0 (k_1/u_0^2 + k_2) + \cos u_0 (k_3/u_0^3 + k_4/u_0 + k_5 u_0) \right. \\ & \left. - k_3/u_0^3 - 2k_5 u_0 \left(\frac{1}{2} \pi |u_0| \right)^{1/2} \left[\frac{1}{2} - S((2|u_0|/\pi)^{1/2}) \right] \right\} d\varphi, \end{aligned} \quad (43)$$

where

$$u_0 = a_0 \cos \varphi, \quad (44)$$

and

$$a_0 = [(2\pi f_s)^2 L] / g = \beta^{1/2} L g / v^2. \quad (45)$$

The constants k_1 – k_5 are $k_1 = -10/63$, $k_2 = 8/189$, $k_3 = -4/9$, $k_4 = -4/63$, and $k_5 = 16/189$. The functions Si, Ci, and S are the sine integral, the cosine integral, and the Fresnel integral, respectively. The variances in Eqs. (40)–(43) have been programmed on a digital computer, using numerical integration techniques. Inspec-

a computer for sea-surface spectra of practical importance. These applications are discussed in Sec. III.

III. APPLICATIONS

A. Variances of the facet movements

In this section the general formulas for the facet statistics are evaluated for a Pierson–Moskowitz sea-surface spectrum of the form

$$F_2(f, \varphi) = F_1(f) [\cos^n(\varphi - \varphi_0)] / x_n, \quad (36)$$

where

$$F_1(f) = \begin{cases} \frac{\alpha g^2}{(2\pi)^4 f^5}, & f > f_s = \frac{g}{2\pi v} \beta^{0.25} \\ 0, & \text{otherwise,} \end{cases} \quad (37)$$

and

$$x_n = \int_{-\pi}^{+\pi} \cos^n \varphi d\varphi, \quad \alpha = 0.0081 \text{ and } \beta = 0.74. \quad (38)$$

The mixing function W used here is

$$W(f, \varphi) = \begin{cases} W_0, & \text{for } |\varphi - \varphi_w| \leq \frac{\pi}{2}, \quad |\varphi_w| \leq \frac{\pi}{2} \\ 1 - W_0, & \text{elsewhere.} \end{cases} \quad (39)$$

The spectrum is inserted into Eqs. (13) to (16). Then the integration over the frequency f is performed, yielding

tion of the equations shows that the variances are functions of the following form:

$$\begin{aligned} \sigma_\epsilon &= f_1(L/v^2), \\ \sigma_z/v &= f_2(L/v^2), \\ \sigma_x/v &= f_3(L/v^2), \\ \sigma_{\epsilon z}/v &= f_4(L/v^2), \end{aligned} \quad (46)$$

and

$$\rho_{\epsilon z} = \frac{\sigma_{\epsilon z}}{\sigma_\epsilon \sigma_z} = f_5(L/v^2).$$

Therefore, the results are shown as a function of L/v^2 rather than the facet length L , thus eliminating the variation of the results as a function of the wind speed v .

The remaining parameters are the direction angle φ_0 , the direction angle φ_w of the mixing function, and the exponent n of the cosine directivity function. In Figs. 3–7 the facet statistics are shown for

$$\varphi_0 = \varphi_w = 0^\circ, 45^\circ, \text{ and } 90^\circ \text{ and } n = 2.$$

For certain applications it is desirable to have analytical expressions for the variances. This can be achieved by approximate solutions of Eqs. (40)–(43) for $a_0 \ll 1$ and $a_0 \gg 1$ and combining the results. They are found in Ref. 7.

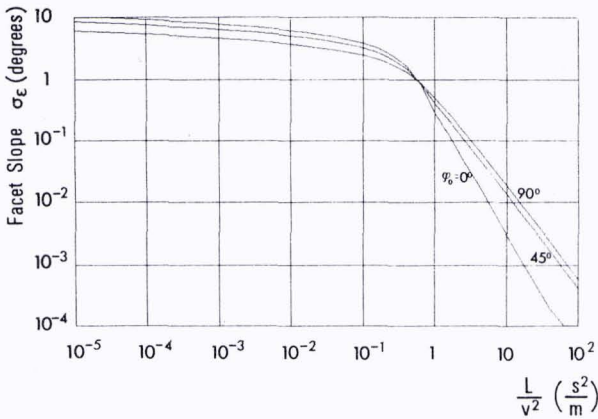


FIG. 3. Facet slope σ_ϵ vs L/v^2 . The parameters are wind direction φ_0 , facet length L , and wind speed v ; directivity exponent: $n = 2$.

B. Calculation of the facet length

The facet length L is calculated following the general procedure of Sec. IIB. The starting equation is Eq. (23), which is evaluated for the Pierson-Moskowitz spectrum. First, the variance σ_h^2 is calculated, employing Eq. (25):

$$\sigma_h^2 = \frac{2\alpha v^4}{\beta x_n g^2} \int_0^\pi \cos^n(\varphi - \varphi_0) \times \left\{ \frac{1}{4} - \frac{1}{u_0^2} - \frac{2}{u_0^4} + \frac{2 \cos u_0}{u_0^4} + \frac{2 \sin u_0}{u_0^3} \right\} d\varphi. \quad (47)$$

The result is given in Fig. 8. The limiting forms for $a_0 \ll 1$ and $a_0 \gg 1$ are interpolated to a formula with the result

$$\frac{L}{\lambda_0} = \left\{ \frac{1}{288} \alpha (3 \cos^2 \varphi_0 + \sin^2 \varphi_0) \right\}^{-1/2} + \frac{4g^2 \beta}{\alpha (v/\lambda_0^{1/2})^4} \Bigg\}^{1/2}. \quad (48)$$

This result relates the surface parameters of wind speed v and wind direction φ_0 and the acoustic wave length λ_0 to the facet length L . Equation (48) is plotted in Fig. 9, together with the exact result obtained by the solution of Eq. (23) with an iterative procedure on the digital computer. The figure shows that the maximum error does not exceed 20%; thus the approximation

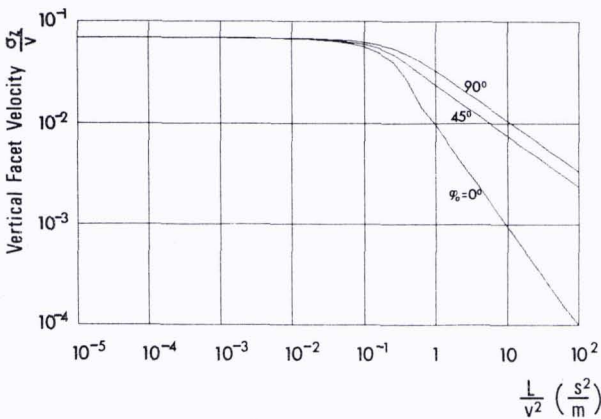


FIG. 4. Vertical facet velocity σ_z/v vs L/v^2 .

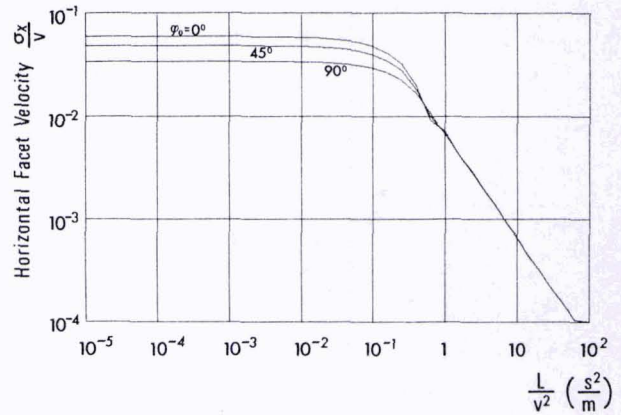


FIG. 5. Horizontal facet velocity σ_x/v vs L/v^2 .

should be sufficient in most cases. It is further seen that the quality number $N = L/\lambda_0$ is always greater than 10; therefore the errors induced by the facets can be considered small.

The same procedure was performed for the exponent $n = 4$ of the directivity law. The result is similar, the only difference being a larger variation of L with the direction angle φ_0 .

C. Resulting Doppler spectra

With the facet statistics being calculated the results for the Doppler spectra will now be discussed. The sea-surface spectrum employed to evaluate Eq. (29) is a modified version of the Scott spectrum¹¹ of the form

$$F_2(f, \varphi) = A_s F_1(f) |\cos \frac{1}{2}(\varphi - \varphi_0)|^{2s}, \quad (49)$$

where

$$s = 5.5 \text{ Hz} / 2\pi f \quad (50)$$

and

$$A_s = \Gamma(2s + 1) / [2^{2s+2} \Gamma^2(s + \frac{1}{2})]. \quad (51)$$

The mixing function is

$$W(f, \varphi) = \frac{B + |\cos \frac{1}{2}(\varphi - \varphi_0)|^{2s}}{2B + |\cos \frac{1}{2}(\varphi - \varphi_0)|^{2s} + |\sin \frac{1}{2}(\varphi - \varphi_0)|^{2s}}, \quad (52)$$

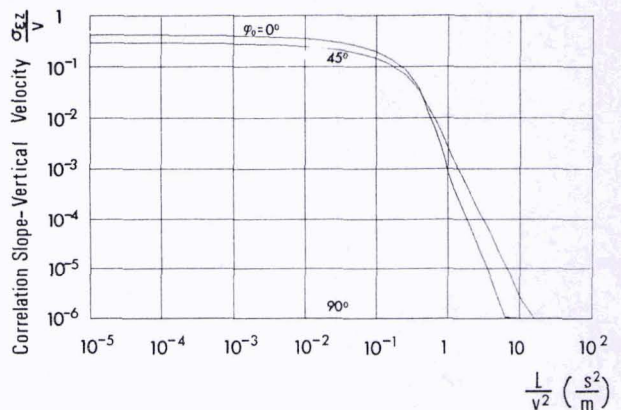


FIG. 6. Correlation between slope and vertical velocity, σ_{ϵ_z}/v vs L/v^2 .

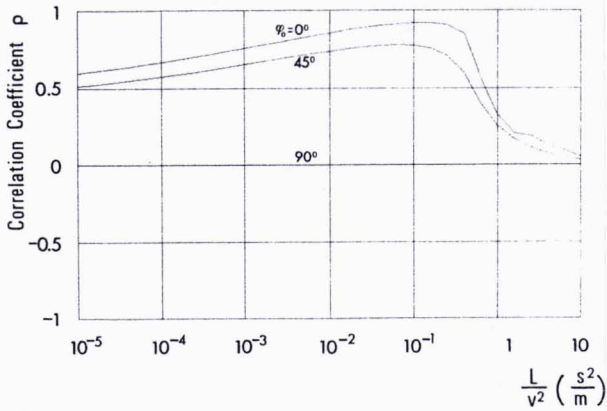


FIG. 7. Correlation coefficient ρ vs L/v^2 .

where

$$B = f/f_g \tag{53}$$

and f_g is a limiting frequency, at which the spectrum becomes more omnidirectional.

This choice of the sea-surface spectra seems to be the best possibility at present. It should be understood, however, that the general result for the Doppler density of backscattered sound can be evaluated for any sea-surface spectrum written in a form used here.

In Fig. 10 the influence of the grazing angle γ_0 , on the Doppler density is demonstrated. The x axis shows the Doppler shift $f - f_0$ in Hertz, the y axis shows the Doppler density $\varphi(f)$ in 1/(Hertz). The angle γ_0 is changed from 2° to 20° , the wind speed is $v = 8$ m/s, the incident acoustic frequency is 3.5 kHz, and the main direction of the surface waves points away from the sound source. This causes an asymmetry in the spectrum, which is explained as follows: The correlation between the facet slope and the facet vertical velocity is negative in this case; this means that a large angle belongs to a negative velocity. This velocity causes negative Doppler shift; as the slope is greater for the negative velocity than for the positive velocity the backscattered energy is greater. In this figure the sea-surface spectrum is

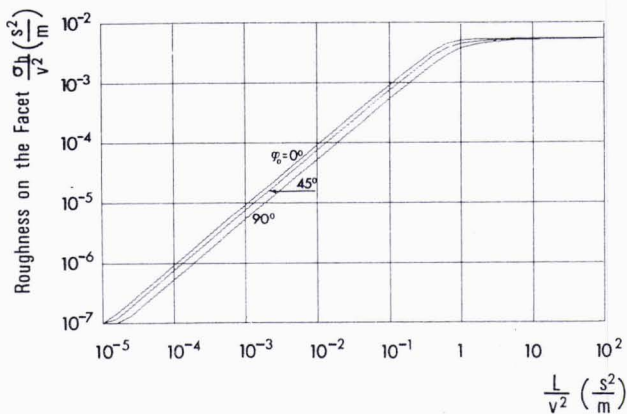


FIG. 8. Roughness on the facet σ_h/v^2 vs L/v^2 .

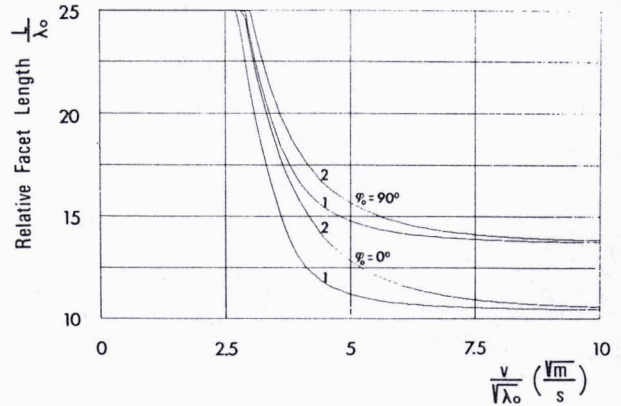


FIG. 9. Relative facet length L/λ_0 vs $v/\sqrt{\lambda_0}$; parameters: wind direction ϕ_0 , facet length L , wind speed v , and acoustic wavelength λ_0 . Directivity exponent $n = 2$. (1) Exact result and (2) approximation.

omnidirectional in the frequency range where resonant scattering occurs, at about 2.7 Hz or 20-cm wavelength. The lack of symmetry is due only to the facet movement. If the orientation of the sea-surface spectrum is 90° off the incident wave vector, this effect does not occur.

The curves depend quite strongly on the limiting frequency f_g , which is especially apparent if f_g tends to infinity, leading to a spectrum that has a directivity up to the highest frequencies. This case is shown in Fig. 11 for the same parameters as in the previous figure. In fact, the figure contains only one branch of the usual two, as only one δ function occurs in the resonant scattering case.

Figure 12 shows the influence of the wind speed for a fully developed sea. The grazing angle γ_0 is 6° , the orientation angle ϕ_0 is 0° , and the acoustic frequency f_0 is 3.5 kHz. The wind speed varies from 2 to 32 m/s in geometrical progression. For low wind speed the facet model is seen to be superfluous, as the Doppler density consists virtually of two δ functions due to the resonant scattering. For high wind speeds, the back-

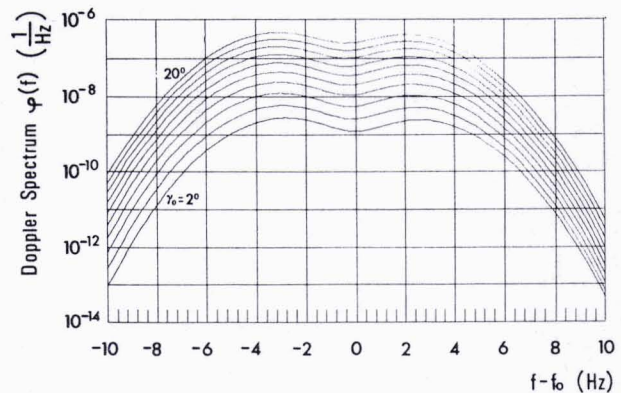


FIG. 10. Doppler spectral density $\varphi(f)$ vs Doppler shift $f - f_0$. Parameters: grazing angle $\gamma_0 = 2^\circ - 20^\circ$, center frequency $f_0 = 3.5$ kHz, wind speed $v = 8$ m/s, wind direction $\phi_0 = 0^\circ$ (downwind), and limiting frequency $f_g = 1$ Hz.

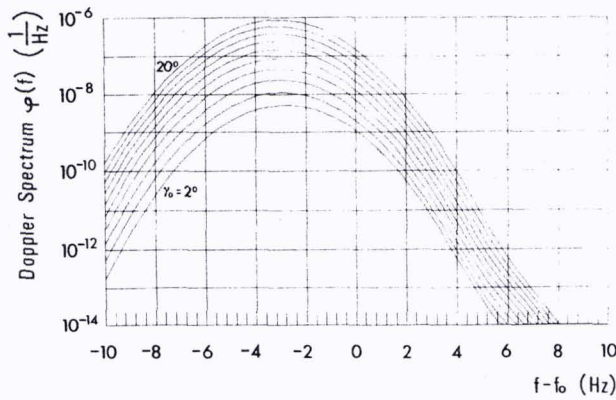


FIG. 11. Doppler spectral density $\phi(f)$ vs Doppler shift $f - f_0$. Parameters as in Fig. 10 except $f_g \rightarrow \infty$.

scattered energy is considerably higher but is spread over a higher frequency range; the backscattered energy at the Bragg frequency does not change considerably.

Figure 13 shows the Doppler density versus the normalized frequency $\Delta f/f_0 = f - f_0/f_0$ for $f_0 = 0.3, 1, 3.3, 10,$ and 33 kHz. For the low frequency $f_0 = 330$ Hz the Rayleigh condition is fulfilled; thus the Doppler spectral density consists of two sharp peaks. With increasing frequency the facets become more important and at the same time the asymmetry of the curves disappears, because the Bragg frequency is shifted to the omnidirectional part of the sea-surface spectrum. The limiting frequency is $f_g = 5$ Hz in this case; this means that for $f_0 = 33$ kHz the resonant frequency is $f_0^* = 8.25$ Hz, and accordingly the spectral density $\phi(f)$ is almost symmetrical.

IV. CONCLUSION

A theoretical model for the Doppler spread of the backscattered acoustic waves from the rough sea surface is developed that makes use of a two-component structure (facet model) of the sea surface.

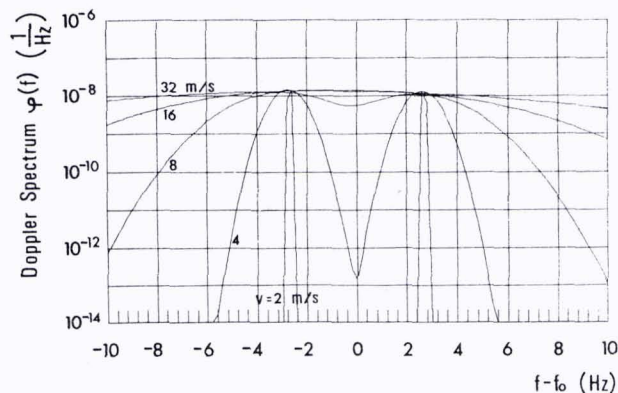


FIG. 12. Doppler spectral density $\phi(f)$ vs Doppler shift $f - f_0$. Parameters: wind speed $v = 2-32$ m/s, center frequency $f_0 = 3.5$ kHz, grazing angle $\gamma_0 = 6^\circ$, wind direction $\phi_0 = 0^\circ$ (downwind), limiting frequency $f_g = 1$ Hz.

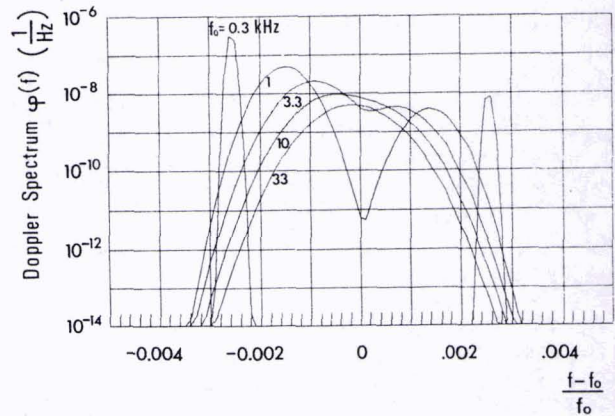


FIG. 13. Doppler spectral density $\phi(f)$ vs normalized Doppler shift $(f - f_0)/f_0$. Parameters: center frequency $f_0 = 0.3-33$ kHz, grazing angle $\gamma_0 = 6^\circ$, wind speed $v = 8$ m/s, wind direction $\phi_0 = 0^\circ$ (downwind), limiting frequency $f_g = 5$ Hz.

The model requires a description of the statistical properties of the sea-surface roughness including the directivity and the mixing of incoming and outgoing waves in one direction as function of frequency. The concept of the mixing function is necessary to obtain asymmetrical Doppler spectra as a function of the wind direction. The parameters of this function need experimental verification; in particular, the optimal value for the limiting frequency is not yet known.

The general result of this paper is a set of formulas for both the facet statistics and the Doppler spectrum in terms of the sea-surface covariance function or the sea-surface spectrum. The results can be used in two ways:

- (1) Measured sea-surface data are used to fit the parameters of analytical spectra such as the Pierson-Moskowitz spectrum or the Scott spectrum.
- (2) Measured spectra are inserted into the general formulas.

The procedure, developed for the choice of the facet length L shows that the quality number $N = L/\lambda_0$, where λ_0 is the acoustic wavelength, is never smaller than 10; thus the error due to finite facet length can be considered small.

The general results for the statistics of the facets are evaluated for a Pierson-Moskowitz spectrum. An approximate closed-form solution is obtained.

For the numerical evaluation of the general result for the Doppler spectral density, a more general sea-surface spectrum due to Scott is employed, which contains the Pierson-Moskowitz spectrum as a special case.

Examples for different wind speeds, wind directions, grazing angles, and acoustic frequencies are calculated via a computer program.

APPENDIX: STATISTICAL SEA-SURFACE DESCRIPTION

The sea surface $h(x, y, t)$ is considered as a three-dimensional process that is assumed to be Gaussian distributed and stationary in space and time. Then the statistical properties of this process are completely described by its covariance function $C(x, y, \tau)$, where x and y are the space lag and τ is the time lag between two points of observation.

The covariance function is related to the three-dimensional wave parameter frequency spectrum $X_3(k_x, k_y, f)$ via the three-dimensional Fourier transform:

$$X_3(k_x, k_y, f) = \int_{-\infty}^{+\infty} \int_{-\infty}^{+\infty} \int_{-\infty}^{+\infty} C(x, y, \tau) \exp[-j2\pi(-k_x x - k_y y + f\tau)] dx dy d\tau, \quad (\text{A1})$$

where both X_3 and C are real-valued functions. In Eq. (A1) f is the frequency and the wave components k_x and k_y are defined as

$$k_x^2 + k_y^2 = k^2 \quad \text{and} \quad k = 1/\lambda, \quad (\text{A2})$$

where λ is the wavelength of the corresponding surface wave and k is the wave parameter. For deep water and surface wavelengths not shorter than about 5 cm the dispersion relation is valid:

$$2\pi f^2 = gk, \quad (\text{A3})$$

where g is the gravitational constant. Then the three-dimensional spectrum $X_3(k_x, k_y, f)$ can be written as

$$X_3(k_x, k_y, f) = X_2(k_x, k_y) W[k_x \operatorname{sgn}(f), k_y \operatorname{sgn}(f)] \times [\delta(f - f^*) + \delta(f + f^*)], \quad (\text{A4})$$

where

$$f^* = [(g/2\pi)(k_x^2 + k_y^2)^{1/2}]^{1/2}. \quad (\text{A5})$$

In Eq. (A4) the function $X_2(k_x, k_y)$ is the wave parameter spectrum. $X_2(k_x, k_y)$ contains the orientational information of the frozen sea surface. The "mixing function" W describes the ratio of incoming and outgoing waves for a given wave vector. The function $W(x, y)$ has the properties

$$0 \leq W(x, y) \leq 1$$

and (A6)

$$W(x, y) = 1 - W(-x, -y).$$

It is used in Eq. (A4) with the complicated argument $W[k_x \operatorname{sgn}(f), k_y \operatorname{sgn}(f)]$ to fulfill the symmetry relations imposed on the wave parameter spectra $X_3(k_x, k_y, f)$ and $X_2(k_x, k_y)$, namely,

$$X_3(k_x, k_y, f) = X_3(-k_x, -k_y, -f) \quad (\text{A7})$$

$$X_2(k_x, k_y) = X_2(-k_x, -k_y)$$

that are necessary to obtain a real covariance function.

Instead of the wave parameter spectrum X_2 the equivalent frequency angle spectrum $F_2(f, \varphi)$ is used in the literature. Defining this function via the normalizing equation

$$\sigma_h^2 = \int_0^{+\infty} \int_{-\pi}^{+\pi} F_2(f, \varphi) df d\varphi = C(0, 0, 0) \quad (\text{A8})$$

the relationship to $X_2(k_x, k_y)$ is

$$F_2(f, \varphi) = \frac{8\pi^2 f^3}{g^2} X_2\left(\frac{2\pi f^2}{g} \cos\varphi, \frac{2\pi f^2}{g} \sin\varphi\right) \quad (\text{A9})$$

or

$$X_2(k_x, k_y) = \frac{g^2}{8\pi^2 f^{*3}} F_2\left(f^*, \arctan \frac{k_x}{k_y}\right), \quad (\text{A10})$$

where again the dispersion relationship of Eq. (A3) is used. $F_2(f, \varphi)$ has the symmetry property

$$F_2(f, \varphi) = F_2(f, \varphi \pm \pi). \quad (\text{A11})$$

In many practical cases the dependence of $F_2(f, \varphi)$ on φ is not known. Then a simple frequency spectrum $F_1(f)$ is introduced via

$$\sigma_h^2 = \int_0^{+\infty} F_1(f) df, \quad (\text{A12})$$

and the relation to F_2 is

$$F_1(f) = 2\pi F_2(f, \varphi), \quad (\text{A13})$$

if F_2 is independent on φ . In this case the mixing function W is set to 0.5 and one obtains the relationship

$$X_3(k_x, k_y, f) = \frac{g^2}{4(2\pi f^*)^3} F_1(f^*) [\delta(f - f^*) + \delta(f + f^*)]. \quad (\text{A14})$$

The above equations are connected to the covariance function C via Eq. (A1). For instance, one obtains for the frequency angle spectrum

$$C(x, y, \tau) = \int_0^{+\infty} \int_{-\pi}^{+\pi} F_2(f, \varphi) \left\{ \cos 2\pi f \tau \cos \left[\frac{(2\pi f)^2}{g} \right. \right. \\ \times (x \cos\varphi + y \sin\varphi) \left. \left. \right] + [2W(f, \varphi) - 1] \sin 2\pi f \tau \right. \\ \left. \times \sin \left[\frac{(2\pi f)^2}{g} (x \cos\varphi + y \sin\varphi) \right] \right\} d\varphi df, \quad (\text{A15})$$

where

$$0 \leq W(f, \varphi) \leq 1$$

and

$$W(f, \varphi) = 1 - W(f, \varphi \pm \pi). \quad (\text{A16})$$

Any other relations are calculated easily from the above equations.

In Ref. 12, a special form of the mixing function is assumed

$$W(f, \varphi) = \begin{cases} 1, & \text{for } |\varphi| \leq \pi/2 \\ 0, & \text{elsewhere.} \end{cases} \quad (\text{A17})$$

Then Eq. (A15) reduces to

$$C(x, y, \tau) = 2 \int_0^{\infty} \int_{-\pi/2}^{+\pi/2} F_2(f, \varphi) \cos \left[2\pi f \tau - \frac{(2\pi f)^2}{g} \right. \\ \left. \times (x \cos \varphi + y \sin \varphi) \right] d\varphi df. \quad (\text{A18})$$

¹H. W. Marsh, "Sound Reflection and Scattering from the Sea Surface," *J. Acoust. Soc. Am.* **35**, 240-244 (1963).

²B. E. Parkins, "Scattering from the Time-Varying Surface of the Ocean," *J. Acoust. Soc. Am.* **42**, 1262-1267 (1967).

³B. F. Kuryanov, "The Scattering from the Time-Varying Surface of the Ocean," *Soviet Phys.—Acoust.* **8**, 252-257 (1963).

⁴W. Bachmann, "Verallgemeinerung und Anwendung der Rayleighschen Theorie der Schallstreuung," *Acustica* **38**, 223-228 (1973).

⁵W. Bachmann, "A Theoretical Model for the Backscattering

Strength of a Composite-Roughness Sea Surface," *J. Acoust. Soc. Am.* **54**, 712-716 (1973).

⁶H. H. Essen, "Wave-Facet Interaction Model Applied to Acoustic Scattering from a Rough Sea Surface," *Acustica* **31**, 107-113 (1974).

⁷H. Schwarze, "A Model for the Doppler Spread of Backscattered Sound from a Composite Roughness Sea Surface," *SACLANTCEN Memorandum*, SM-86 (1976).

⁸R. H. Clarke, "Theory of Acoustic Propagation in a Variable Ocean," *SACLANTCEN Memorandum* SM-28.

⁹R. J. Urick, *Principles of Underwater Sound for Engineers* (McGraw-Hill, New York, 1967), Chap. 8, p. 188.

¹⁰Lord Rayleigh, *The Theory of Sound* (Dover, New York, 1945), Vol. II, p. 89.

¹¹J. R. Scott, "Some Average Wave Length on Short-Crested Seas," *Q. J. R. Meteorol. Soc.* **95**, 621-634 (1969).

¹²G. Neumann and W. J. Pierson, *Principles of Physical Oceanography* (Prentice-Hall, Englewood Cliffs, NJ (1966).

INITIAL DISTRIBUTION

<u>MINISTRIES OF DEFENCE</u>	Copies	<u>SCNR FOR SACLANTCEN</u>	Copies
MOD Belgium	2	SCNR Belgium	1
DND Canada	10	SCNR Canada	1
CHOD Denmark	8	SCNR Denmark	1
MOD France	8	SCNR Germany	1
MOD Germany	15	SCNR Greece	1
MOD Greece	11	SCNR Italy	1
MOD Italy	10	SCNR Netherlands	1
MOD Netherlands	12	SCNR Norway	1
CHOD Norway	10	SCNR Portugal	1
MOD Portugal	5	SCNR Turkey	1
MOD Turkey	5	SCNR U.K.	1
MOD U.K.	16	SCNR U.S.	2
SECDEF U.S.	61	SECGEN Rep.	1
		NAMILCOM Rep.	1
 <u>NATO AUTHORITIES</u>		 <u>NATIONAL LIAISON OFFICERS</u>	
Defence Planning Committee	3	NLO Canada	1
NAMILCOM	2	NLO Denmark	1
SACLANT	10	NLO Germany	1
SACLANTREPEUR	1	NLO Italy	1
CINCWESTLANT/COMOCEANLANT	1	NLO U.K.	1
COMIBERLANT	1	NLO U.S.	1
CINCEASTLANT	1		
COMSUBACLANT	1	<u>NLR TO SACLANT</u>	
COMMAIREASTLANT	1	NLR Belgium	1
SACEUR	2	NLR Canada	1
CINCNORTH	1	NLR Germany	1
CINCSOUTH	1	NLR Greece	1
COMNAVSOUTH	1	NLR Italy	1
COMSTRIKFORSOUTH	1	NLR Norway	1
COMEDCENT	1	NLR Portugal	1
COMMARAIRMED	1	NLR Turkey	1
CINCHAN	1		
		Total initial distribution	232
		SACLANTCEN Library	10
		Stock	38
		Total number of copies	280